Nanozyme chemiluminescence paper test for rapid and sensitive detection of SARS-CoV-2 antigen

Dan Liu [a],[1], Chenhui Ju [a],[1], Chao Han [b],[c],[1], Rui Shi [b], Xuehui Chen [a], Demin Duan [a], Jinghua Yan [b],[d], Xiyun Yan [a],[*]

[a] CAS Engineering Laboratory for Nanozyme, Institute of Biophysics, Chinese Academic of Science, Beijing, 100101, China
[b] CAS Key Laboratory of Microbial Physiological and Metabolic Engineering, Institute of Microbiology, Chinese Academy of Sciences, Beijing, 100101, China
[c] University of Chinese Academy of Sciences, Beijing, 100049, China
[d] Savaid Medical School, University of Chinese Academy of Sciences, Beijing, 100049, China

ABSTRACT

COVID-19 has evolved into a global pandemic. Early and rapid detection is crucial to control of the SARS-CoV-2 transmission. While representing the gold standard for early diagnosis, nucleic acid tests for SARS-CoV-2 are often complicated and time-consuming. Serological rapid antibody tests are characterized by high rates of false-negative diagnoses, especially during early infection. Here, we developed a novel nanozyme-based chemiluminescence paper assay for rapid and sensitive detection of SARS-CoV-2 spike antigen, which integrates nanozyme and enzymatic chemiluminescence immunoassay with the lateral flow strip. The core of our paper test is a robust Co–Fe@hemin-peroxidase nanozyme that catalyzes chemiluminescence comparable with natural peroxidase HRP and thus amplifies immune reaction signal. The detection limit for recombinant spike antigen of SARS-CoV-2 was 0.1 ng/mL, with a linear range of 0.2-100 ng/mL. Moreover, the sensitivity of test for pseudovirus could reach 360 $TCID_{50}$/mL, which was comparable with ELISA method. The strip recognized SARS-CoV-2 antigen specifically, and there was no cross reaction with other coronaviruses or influenza A subtypes. This testing can be completed within 16 min, much shorter compared to the usual 1-2 h required for currently used nucleic acid tests. Furthermore, signal detection is feasible using the camera of a standard smartphone. Ingredients for nanozyme synthesis are simple and readily available, considerably lowering the overall cost. In conclusion, our paper test provides a high-sensitive point-of-care testing (POCT) approach for SARS-CoV-2 antigen detection, which should greatly facilitate early screening of SARS-CoV-2 infections, and considerably lower the financial burden on national healthcare resources.

1. Introduction

Coronavirus Disease 2019 (COVID-19) has developed into a global pandemic, causing over 1 Million deaths by the end of October 2020. A novel RNA virus named severe acute respiratory syndrome coronavirus 2 (SARS-CoV-2) is responsible for this pandemic (Wu et al. 2020; Zhou et al. 2020). SARS-CoV-2 is highly infectious and spreads through human-to-human interaction mediated mainly by airborne droplets. SARS-CoV-2 mainly infects through the upper respiratory tract and can cause severe symptoms including fever, dry cough, fatigue or progressive dyspnea, and in extreme cases death (Hu et al. 2020). One major concern for healthcare systems is to discover infections early during the incubation period, as well as asymptomatic carriers, making a rapid and reliable test critical for successful control of the pandemic (Mei et al. 2020). To date, vaccines for COVID-19 are still awaiting approval for use across entire populations. Therefore, both early detection and early quarantine are the most effective ways to control this pandemic (Wiersinga et al. 2020).

Pathogenic tests play a vital role in diagnosis of COVID-2019. At present, nucleic acid tests based on fluorescence PCR or isothermal nucleic acid amplification are primarily used for early diagnosis of COVID-19 (Grant et al. 2020; Huang et al. 2020). However, nucleic acid testing requires biosafety laboratories as well as skilled personnel. Moreover, nucleic acid tests require RNA extraction, reverse

---

transcription, gene amplification and data analysis, taking at least 1–2 h, rendering such tests unsuitable for field and immediate screening. Due to the high cost, it is also out of reach for many less well-endowed communities or health care systems, especially in developing countries. Simple, rapid and reliable detection reagents for SARS-CoV-2 are still urgently required.

Antibody testing is another approach assisting nucleic acid diagnosis (Xiao et al. 2020). Colloidal gold paper and fluorescent chromatography paper have also been rapidly developed for COVID-19 diagnosis (Amanat et al. 2020). Currently available antibody tests detect IgM or/and IgG antibodies present in blood samples (Jia et al. 2020; Li et al. 2020b). However, serological antibody testing cannot replace pathogenic testing. Critically, antibodies are generated only 10–15 days past virus exposure (Zhao et al. 2020), and therefore it is not suitable for early screening and diagnosis of COVID-19 (Shi et al. 2020b).

WHO has recently released interim guidance that the use of rapid antigen diagnostic tests that meet at least 80% sensitivity and 97% specificity may be considered to diagnose active SARS-CoV-2 infection (WHO 2020). Recently, published studies from different countries evaluating commercial and in-house Antigen tests for SARS-COV-2 showed high levels of specificity (from 99.5 to 100 %), albeit with a wide range of sensitivity (30 %–93.9 %) (Cerutti et al. 2020; Porte et al. 2020; Scohy et al. 2020). Therefore, considerable efforts for improving antigen test performance are currently undertaken.

In our previous study, we reported a nanozyme colorimetric strip test for Ebola virus detection, which is based on Fe_3O_4 nanozyme-catalyzed chromogenic reaction (Duan et al. 2015). Nanozymes are nanomaterials endowed with intrinsic enzyme-mimicking activity (Gao et al. 2007), which can be used for enzymatic biosensors. Although previous studies have reported the applications of nanozyme in immunoassay, these works achieved signal amplification based on a chromogenic reaction (Cheng et al. 2017; Duan et al. 2015), rather than chemiluminescence. Enzymatic chemiluminescence analysis (CLIA) has been widely used in immunodiagnosis due to its higher sensitivity and wider linear range compared with enzyme-linked immunosorbent assay (ELISA). However, traditional chemiluminescence detection depends on the use of expensive precision instruments, which are only suitable for central clinical laboratories. Moreover, traditional CLIA is based on a natural protease, such as natural horseradish peroxidase (HRP) or alkaline phosphatase (ALP), all of which are characterized by drawbacks, including low storage stability and complex preparation procedures. One research has reported the application of gold nanoparticles in chemiluminescent lateral flow assay, however, the design was based on the catalysis of natural HRP (Deng et al. 2018), which has poor stability and limits the practical use in field test.

Here, we developed a nanozyme chemiluminescence paper test for rapid, high-sensitive and portable detection of SARS-CoV-2 spike antigen (S antigen). We have established a rapid detection platform based on a Co–Fe@hemin-peroxidase nanozyme as an alternative to HRP, which combines traditional CLIA with lateral flow assay. As a novel point-of-care approach, this nanozyme chemiluminescence paper test will be of considerable benefit to rapidly screening of suspected SARS-CoV-2 infections, especially during the early stages of viral infections.

2. Materials and methods

2.1. Reagents and materials

$FeCl_3.6H_2O$, $CoCl_2.6H_2O$, Poly (acrylic acid), Hemin, TMB, HRP, EDC, NHS, BSA, DAB and hydrogen peroxide (H_2O_2) were purchased from Sigma-Aldrich Co. LLC. (Shanghai, China). Polyethylene glycol was purchased from Yeasen Biotech Co., Ltd. Sodium acetate was purchased from Sinopharm Chemical Reagent Co., Ltd (Shanghai, China). Luminol substrate was purchased from Macklin Biochemical Co., Ltd (Shanghai, China). Luminunc™ MicroWell 96 plates were purchased from Nunc (Denmark). Nitrocellulose membrane was purchased from Sartorius

(Germany). Fiberglass pads, absorbent pads and PVC plastic boards were purchased from Shanghai Kinbio Tech. Co. Ltd. TP52, RP01 antibodies, ELISA reagent kit for spike antigen, SARS-CoV S-RBD, MERS-CoV S-RBD, HCoV-HKU1 and HCoV-OC43 spike protein were purchased from Sino Biological Inc. (Beijing, China). Ab1 and Ab2 antibodies were provided by courtest of Prof. Benfen Shen from Academy of Military Medical Sciences. Influenza A subtypes H1N1 (A/California/04/2009 and A/Puerto Rico/8/34 strains), H3N2 (A/Duck/Eastern China/866/ 2003), H5N1 (A/Mallard/Huadong/S/2005), H7N9 (A/Chicken/ Eastern China/JD/2017) were supplied by courtesy of Prof. George Fu Gao's lab in the Institute of Microbiology (Beijing, China) and Prof. Lizeng Gao's lab in the Institute of Biophysics (Beijing, China). Influenza A subtypes were propagated in 10-d-old specific pathogen-free (SPF) embryonated chicken eggs, the allantoic fluid was harvested 48–72 h later. The influenza A virus antigen detection kits were purchased from Wondfo Inc. (Guangzhou, China).

2.2. Preparation of Co–Fe@hemin-peroxidase nanozyme

Firstly, Co–Fe nanoparticles (Co–Fe NPs) with carboxyl modification were synthesized using a hydrothermal method with some modifications (Deng et al. 2005; Zhuang et al. 2012). In brief, 7.2 g of $FeCl_3.6H_2O$ and 2.1 g of $CoCl_2.6H_2O$ were dissolved in 400 mL polyethylene glycol. Next, 30 g of sodium acetate (NaAc) and 3 g of poly (acrylic acid) were added under vigorous stirring. The solution was transferred into the high-temperature autoclave and heated at 200°C for 12–14 h. The synthesized nanoparticles were then gathered by magnetic separation and washed with ethyl alcohol and deionized water. Subsequently, 40 mg of Co–Fe NPs prepared above were added into 400 mL NaAc solution. Next, 16 mg of hemin was dropwise added into the reaction system. After continuous stirring for 2 h at room temperature, the Co–Fe@hemin nanocomposites were purified by magnetic separation and washed with deionized water. The yield of nanocomposites was calculated according to the mass of the solid-state materials after thoroughly drying off.

2.3. Characterization of Co–Fe@hemin-peroxidase nanozyme

Transmission electron microscopy (TEM) images were obtained using a Tecnai Sprit microscope instrument operating at 120 KV (FEI Inc., America). The scanning electron microscopy (SEM) images were taken on a SU8020 microscope instrument (Hitachi, Japan). The hydrate particle size of Co–Fe@hemin nanozyme was measured using a 271-DPN dynamic light scattering (DLS) instrument. The UV–Vis absorbance spectra were scanned using a U-3900 absorption spectrophotometer (Hitachi, Japan) in a wavelength range of 200–600 nm. Surface carboxyl group modification was characterized using Thermogravimetric-Differential Scanning Calorimeter (TG-DSC) analysis using STA449F3 Jupiter (Netzsch, Germany) at a heating rate of 10°C/min under N_2 protection. The elemental analysis was performed using Energy Dispersive Spectroscopy (EDS) equipped in a SEM microscope instrument. The valence state of elements was tested using X-ray photoelectron spectroscopy (XPS, Thermo Escalab 250Xi, USA). The binding energies and peaks were referenced to the C 1s at 284.8 eV.

2.4. Catalytic activity evaluation of Co–Fe@hemin-peroxidase nanozyme

The peroxidase activity of Co–Fe@hemin-peroxidase nanozyme was measured according to a previously published procedure (Jiang et al. 2018). In brief, nanoparticles of different concentrations were added to 2 mL HAc/NaAc buffer (0.2 M, pH 3.6), then 100 μl TMB and 100 μl H_2O_2 (30% wt/vol) were added to the cuvette. The absorbance at 652 nm was measured for 1 min at the temperature of 37°C, and the reaction-time curve was plotted. The specific activity (SA, U/mg) of nanozyme was calculated according to the formula in literature. The chemiluminescence catalytic activity was measured with an EnVision Multilabel plate reader (PerkinElmer) using a liquid auto-injection

system and luminol substrate. The maximum chemiluminescent intensities catalyzed by Co–Fe@hemin-peroxidase nanozyme were measured at different pH (pH 2–14), temperature pretreatment (4–100°C) and different concentrations of H_2O_2, with HRP as a positive control. Moreover, the intermediate reactive oxygen species in the reaction system were monitored by using electron spin resonance (ESR) spectroscopy and the spin trap agent, 5,5-dimethyl-1-pyrroline-N-oxide (DMPO).

2.5. Recombinant spike antigen, antibody and pseudovirus preparation

The recombinant antigen is a receptor binding domain of the SARS-CoV-2 spike protein (S-RBD, located in the S1 subunit of spike protein) with fusion of His-tag (Wrapp et al. 2020). A cDNA sequence encoding S-RBD was expressed containing both N-terminal natural signal peptide as well as a 6 × His tag at the C-terminus, after transfection into HEK293 cells. After 3 days, supernatants were collected and soluble protein was sequentially purified using HisTrap HP column and Superdex 200 column. The concentration of S-RBD protein was determined using a BCA assay kit (Pierce). The purity of the recombinant protein was analyzed by sodium dodecyl sulfate-polyacrylamide gel electrophoresis (SDS-PAGE). Aliquoted proteins were stored at −20°C ~ −80°C until further use.

Humanized anti-spike antibodies were generated by sorting single memory B cells as previously reported (Shi et al. 2020a). Briefly, peripheral blood mononuclear cells from convalescent COVID-19 patients were incubated with His-tagged S-RBD at 100 nM before staining with anti-CD3, anti-CD16, anti-CD235a, anti-CD19, anti-CD38, anti-CD27 and anti-His antibodies. Antigen-specific memory B cells were identified by the following markers: CD3⁻, CD16⁻, CD235a⁻, CD38⁻, CD19⁺, CD27⁺, hIgG⁺ and His⁺, and sorted into 96-well PCR plates with single cell per/well. The genes encoding Ig VH and VL chains were amplified by 5'RACE and nested PCR. The variable regions of these genes were then cloned into the human IgG1 constant region to generate full-length monoclonal antibodies, which were then expressed and purified by conventional methods. The antibody binding affinity for S-RBD was evaluated by BIAcore 8K.

Pseudoviruses of SARS-CoV-2 were provided by the National Institutes for Food and Drug Control (Beijing, China). Pseudoviruses were prepared as described in literature (Li et al. 2020a; Nie et al. 2020). In brief, the spike gene of SARS-CoV-2 from Wuhan-Hu-1 strain (GenBank: MN908947) was cloned into plasmid pcDNA3.1 to construct the pseudo-SARS-CoV-2. The titration of pseudo-SARS-CoV-2 was carried out as described previously (Ma et al. 2019).

2.6. Preparation of nanozyme chemiluminescence test paper

Anti-S-RBD antibody pairs were screened using ELISA method and nanozyme colorimetric strips (Duan et al. 2015). The preparation of nanozyme chemiluminescence test paper resembles the colloidal gold strip with further modifications. The nanozyme chemiluminescence test paper constitutes a PVC backing plate, an absorbing pad, a sample pad, a nitrocellulose membrane, and a conjugate pad. First, the nanozyme chemiluminescent probes conjugated with detection antibody of S-RBD (S-dAb) were prepared by chemical coupling of the carboxyl group using EDC/NHS agents. The labeled nanozyme probes were stored in modified TB buffer containing 5% BSA. The nanozyme probes were dispensed on the pretreated conjugate pad using a BioDot dispensing equipment. The paired capture antibody of S-RBD (S-cAb) was immobilized on a nitrocellulose membrane at 1.8 mg/mL to form the test line (T-line), as well as the anti-human IgG antibody (1.5 mg/mL) as the control line (C-line). Next, the above conjugate pad, nitrocellulose membrane, sample pad and absorbing pad were assembled on the PVC backing plate and followed by complete drying at 37°C for 1–2 h. The paper boards were cut into 4 mm-wide strips. Finally, the strips were packed into clamp slots and stored at room temperature. The solid chemiluminescence substrate, excitation agent and dissolving buffer were stored in plastic ampoule bottles at room temperature.

2.7. Rapid testing of recombinant SARS-CoV-2 spike antigen

To develop the rapid nanozyme chemiluminescence paper test, recombinant S-RBD antigen of SARS-CoV-2 was used to evaluate the sensitivity of nanozyme chemiluminescence paper test. 100 μl of the sample containing S-RBD protein in the sample dilution buffer was loaded onto the sample pad. The liquid sample flows through the conjugate pad and then the target analytes were recognized specifically by nanozyme probes to form immunocomplexes. Along with lateral flow, nanozyme complexes were captured by S-dAb and aggregated at T-line. Nanozyme probes without antigen combination were found to bind with the anti-IgG antibody at C-line, producing a brown color signal. Following a chromatography step of 15 min, the luminol substrate and excitation agent were dissolved and added onto the detection membrane. The chemiluminescent signals of T-line and C-line were instantly captured by using either a smartphone camera or CCD imaging system (Clinx MiniChemi). Simultaneously, the sensitivity of ELISA detection for S-RBD antigen was evaluated by the commercial ELISA kit according to the manufacturer's instructions. Moreover, the recombinant spike proteins of other human coronaviruses (SARS-CoV, MERS-CoV, HCoV-HKU1 and HCoV-OC43) were detected to validate specificity.

2.8. Rapid testing of pseudo-SARS-CoV-2

The serially diluted pseudoviruses were detected using nanozyme chemiluminescence strip as well as ELISA according to the method described above. Moreover, different strains of Influenza A were detected using nanozyme chemiluminescence strip and commercial antigen detection kit. The allantoic fluid with Influenza A was completely inactivated by 0.3% (wt/vol) formaldehyde at 4°C for 24–48 h (Oie. 2015). The pseudo-SARS-CoV-2 and active Influenza A viruses-related operations were carried out inside a Class II biological safety cabinet. Inactive Influenza A viruses were handled under normal experimental conditions.

3. Results

3.1. Characterization of Co–Fe@hemin-peroxidase nanozyme

Co–Fe@hemin-peroxidase nanozyme is a type of nanomaterial that possesses peroxidase-mimicking activity. We synthesized this nanozyme based on Co–Fe NPs with a high yield (~85%). To characterize the morphology and microstructure of Co–Fe@hemin nanozyme, we performed both TEM and SEM analysis. As shown in Fig. 1A and B, the Co–Fe@hemin nanozymes resemble spherical particles, characterized by an average diameter of approx. 80 nm. DLS analysis showed that the mean hydrated diameter of our nanozyme spheres was approx. 100 nm (Fig. 1C). The UV–Vis spectrum of Co–Fe@hemin-peroxidase nanozyme exhibited two absorption peaks, corresponding to the characteristic peaks of Co–Fe nanoparticles and hemin molecules (Fig. 1D). Using this absorption spectrum, we verified that the hemin modification was present on the surface of Co–Fe@hemin nanozyme. Next, we analyzed the surface carboxyl group modification of Co–Fe@hemin nanozyme using TG-DSC (Fig. S1 A). Furthermore, element composition and content analysis by EDS indicated that the Fe/Co atomic ratio of Co–Fe@hemin is 13:1 (the ratio is 3:1 for Co–Fe NPs) (Fig. S1 B). On the basis of XPS spectra, the binding energies of Fe 2p, Co 2p and O 1s of Co–Fe@hemin nanozyme was identified, referenced to the C 1s peak at 284.8 eV (Fig. S1 C-F).

3.2. Evaluation of the catalytic activity of the Co–Fe@hemin nanozyme

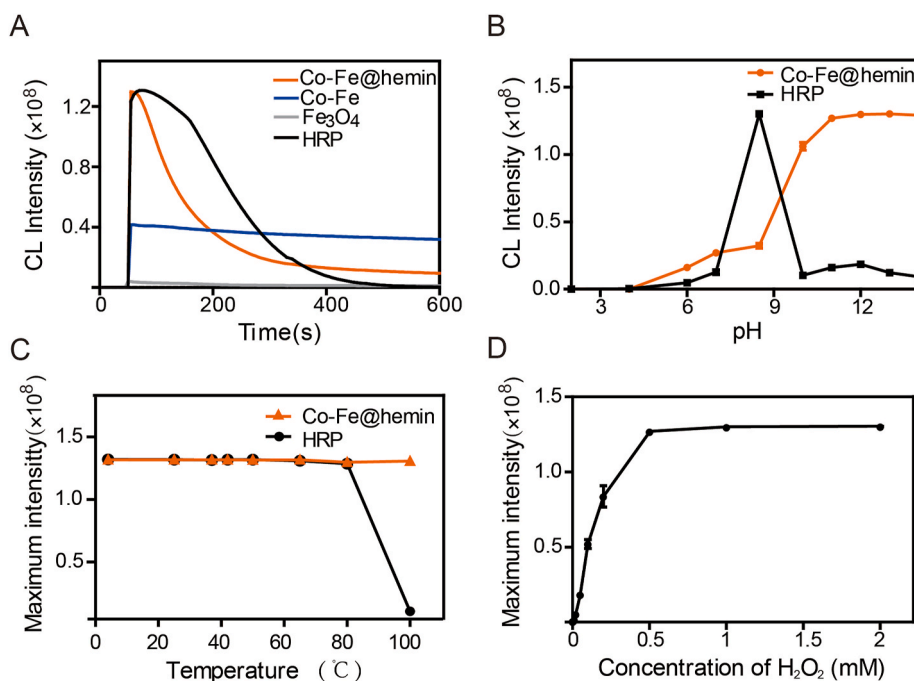Peroxidase activity of our Co–Fe@hemin nanozyme was determined
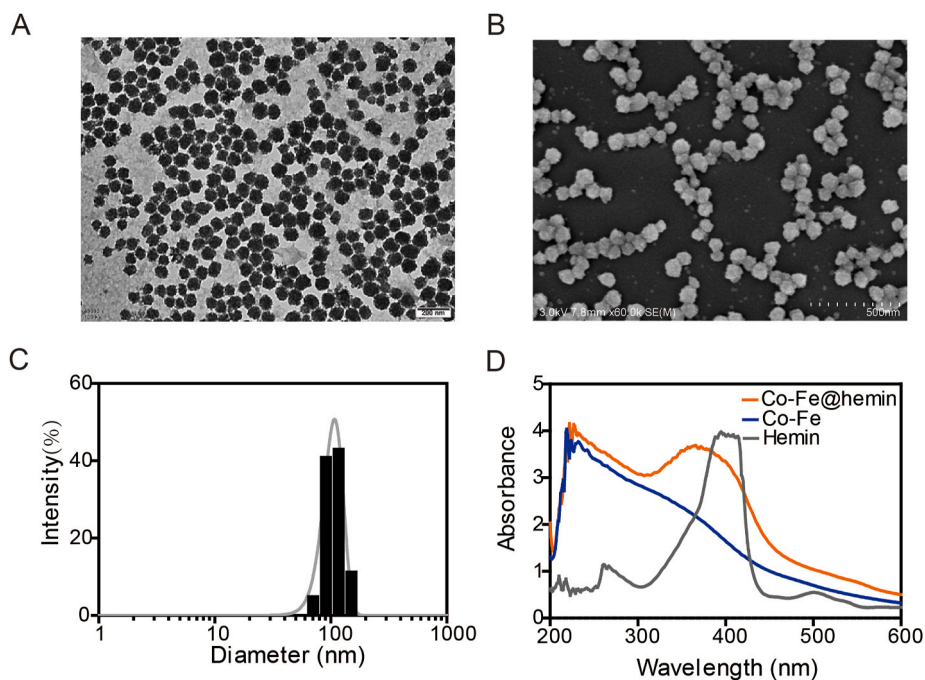
Fig. 1. Characterization of Co–Fe@hemin-peroxidase nanozyme. (A) TEM image of Co–Fe@hemin. (B) SEM image of Co–Fe@hemin. (C) Dynamic light scattering (DLS) analysis. (D) The UV–Vis absorbance spectrum of Co–Fe@hemin, Co–Fe NPs and hemin.

by the specific activity (SA, U/mg) according to procedures established in the literature (Jiang et al. 2018). TMB is one of the chromogenic substrates for HRP. As shown in Fig. S2 A, the catalytic activity of Co–Fe@hemin in TMB chromogenic reaction was 69.915 U/mg, which is higher than Co–Fe NPs (9.836 U/mg) and Fe_3O_4 NPs (5.40 U/mg, data not shown). Next, the chemiluminescence catalytic properties of Co–Fe@hemin nanozyme for luminol substrate was evaluated using an EnVision Multilabel plate reader. The chemiluminescence signals of 1 μg Co–Fe@hemin and HRP were captured in the presence of excitation

agent H_2O_2 under optimal conditions. As shown in Fig. 2A, the maximum chemiluminescent intensity of Co–Fe@hemin was comparable to that of HRP, while showing a three-fold increase over than that of Co–Fe NPs. In comparison, the catalytic chemiluminescence activity of Fe_3O_4 NPs was found to be lower than expected. Moreover, the catalytic chemiluminescence activity of Co–Fe@hemin nanozymes with different sizes were evaluated. Large nanoparticles (160 nm) showed lower chemiluminescence catalytic activity and faster signal decay rate. Nanozymes at the 50 nm and 80 nm scale perform better in

Fig. 2. Catalytic activity of Co–Fe@hemin-peroxidase nanozyme. (A) Chemiluminescence curve for luminol-H_2O_2 system. (B) Effects of pH on chemiluminescence catalytic activity of Co–Fe@hemin and HRP. (C) Effects of temperature on chemiluminescence catalytic activity of Co–Fe@hemin and HRP. (D) Effects of H_2O_2 concentration on Co–Fe@hemin-luminol system. Data were collected in triplicates.

chemiluminescent catalysis (Fig. S2 B).

The Co–Fe@hemin nanozyme displayed high chemiluminescent catalytic activity (the maximum intensity exceeds 8×10^7) at the pH range from 9 to 14, demonstrating that our nanozyme tolerate alkaline conditions (Fig. 2B). In comparison, natural HRP only achieved its maximum catalytic activity for luminol substrate at pH 8.5, and significantly decreased as the pH increased or decreased. Due to a lack of alkaline excitation agent for luminol substrate, both nanozyme and HRP displayed low chemiluminescent catalytic activity in acidic pH. As shown in Fig. 2C (Fig. S3), temperature pretreatment at 4°C–100°C for 2 h failed to affect the catalytic activity of Co–Fe@hemin nanozyme. In contrast, HRP was inactivated after heat pretreatment above 80°C. Together, these results clearly showed that our nanozyme is more robust than HRP, especially under extreme pH and temperature conditions.

Next, we investigated the reaction parameters of H_2O_2 in Co–Fe@hemin-luminol catalytic system. As shown in Fig. 2D, the maximum chemiluminescent intensity increased with the concentration of H_2O_2 at the range of 0.2 μM to 2 mM, reaching the plateau phase above a concentration of 1 mM. Moreover, we monitored superoxide anion radical ($O_2^{-\bullet}$) generation in Co–Fe@hemin-H_2O_2 system under alkaline conditions using the ESR technique. Using DMPO as a trapping agent, we detected a typical ESR signal of the adduct of DMPO with superoxide anion radical (DMPO-$O_2^{-\bullet}$) (Fig. S2 C). We used the peak height as a measure of the concentration of the superoxide anion radical produced in the system. The concentration of $O_2^{-\bullet}$ radical produced by Co–Fe@hemin-H_2O_2 system was higher than that of Co–Fe NPs. Together, these findings indicated that luminol was oxidized by $O_2^{-\bullet}$ radicals generated by the reaction of Co–Fe@hemin with H_2O_2, suggesting a possible mechanism of nanozyme-catalyzed chemiluminescence.

3.3. Design of the nanozyme chemiluminescence paper test

After successfully validating the different core parts of our novel testing platform, we next designed the nanozyme chemiluminescence paper test. Fig. 3A depicts the design of our nanozyme chemiluminescence paper test for SARS-CoV-2 S-RBD antigen. Our paper test is based on the principle of a double antibody sandwich-lateral flow immunoassay. First, Co–Fe@hemin nanozyme chemiluminescence probes labeled with S-dAb were dispersed onto the conjugate pad. Along with the lateral flow of the sample, nanozyme probes combined with S-RBD and S-cAb, forming the sandwich immunocomplexes. The nanozyme probes possess high peroxidase activity, and thus catalyze luminol substrate in the presence of H_2O_2 under alkaline condition, generating chemiluminescence signals. This chemiluminescent signal is then captured by a smartphone camera or CCD and analyzed using Image-Pro Plus software. The well-established testing can be completed within 16 min. The chemiluminescent intensity ratio of T-line to C-line is positively correlated with the concentrations of S-RBD antigen. Due to the small bonding surface of S-RBD antigen and sequence differences from other β-coronaviruses (such as HCoV-HUK1 and HCoV-OC43) (Liu et al. 2020), it is unlikely that cross-reactivity will occur for non-target antigen.

To identify those antibody pairs best suited for antigen detection, we firstly prepared and purified the recombinant S-RBD protein. As shown in Fig. S4, the purity of S-RBD protein was higher than 98% as determined by SDS-PAGE. We then screened a series of anti-spike antibodies using ELISA. Among the six antibodies tested, clones GH4, CB6, TP52 and RP01 exhibited high binding activity for recombinant S-RBD protein (Fig. 3B). Subsequently, we prepared the nanozyme probes labeled with either CB6 or RP01 antibody, and tested with strips immobilized with GH4, RP01 or TP52 as capture antibodies. As shown in Fig. 3C, the CB6 and GH4 pair performed best in S-RBD detection. Other clone pairings resulted in problematic combinations, suggesting that these antibodies recognize either identical or crossed antigenic epitopes. Thus, CB6 was confirmed as a detection antibody and GH4 as a capture antibody in nanozyme chemiluminescence paper test.
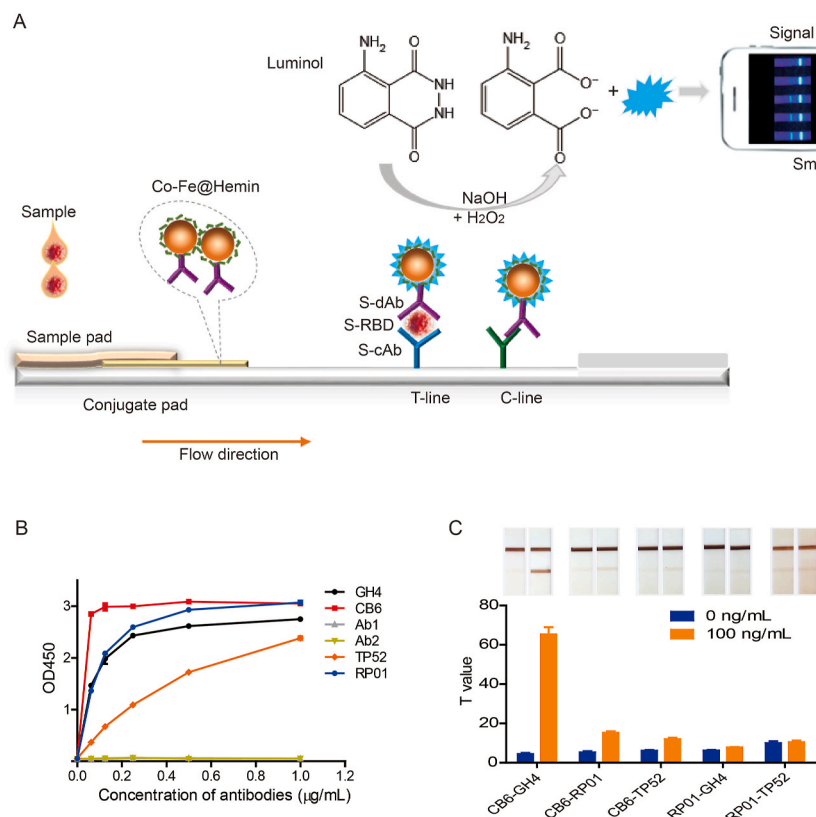
Fig. 3. Design of the nanozyme chemiluminescent paper test. (A) Schematic illustration of the nanozyme chemiluminescence paper test for SARS-CoV-2 S-RBD antigen. Recognition, separation and catalytic amplification by nanozyme probes. (B) ELISA analysis of antibodies binding activity for S-RBD protein. (C) Screening of paired antibodies using nanozyme colorimetric strip. Positive signal was evaluated by 100 ng/mL of S-RBD protein. Sample dilution buffer was used as the negative control. Data were collected in triplicates.
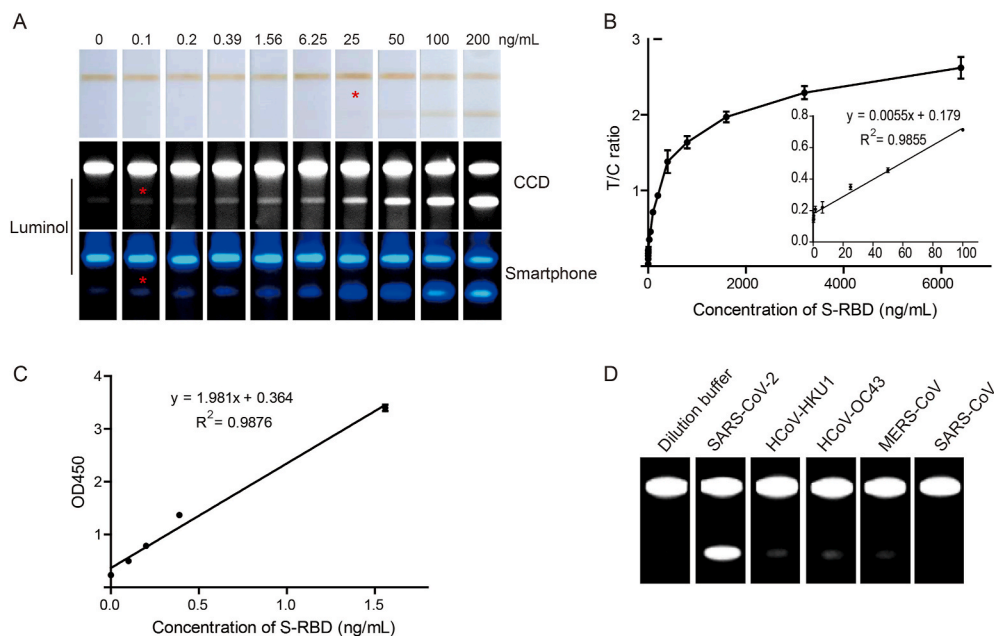
3.4. Rapid testing of recombinant SARS-CoV-2 spike antigen

Using the CB6 and GH4 antibody pair, the nanozyme chemiluminescence test strips for spike antigen were manufactured. To assess the sensitivity of our test, a serial dilution of S-RBD protein samples were prepared. Following a chromatography procedure at room temperature for 15 min, the color signals of T-line were observed by naked eyes at a concentration higher than 25 ng/mL. Next, the luminol substrate was dissolved and added. The chemiluminescent signal was instantly captured using a CCD or smartphone camera in a dark environment (Fig. 4A). Next, the chemiluminescent signal intensity was analyzed using Image-Pro Plus software. The calibration curve of the antigen test was plotted as shown in Fig. 4B. Results showed that the test detected as little as 0.1 ng/mL of S-RBD protein. The detection limit for S-RBD was defined as $\overline{X}$ + 3SD ($\overline{X}$: mean of the negative control, SD: standard deviation) value. The linearity of the test was identified as ranging from 0.2 to 100 ng/mL, with a correlation coefficient of 0.9855 (Fig. 4B). As the parallel test using ELISA, S-RBD antigen was detectable at 0.1 ng/mL, with a linear calibration curve ranging from 0.1 to 1.56 ng/mL (Fig. 4C). The sensitivity of the nanozyme chemiluminescence paper test of S-RBD protein was similar to that of ELISA; however, the linear range of the paper test was found to be at least 32-fold wider than ELISA. To evaluate the reproducibility of nanozyme chemiluminescence strip test, we repeated the test of S-RBD protein at 6.25 ng/mL and 100 ng/mL (n = 10). The Coefficient of Variation (CV) of T/C was calculated according to the formula: CV = standard deviation/mean × 100%. The Coefficient of Variation (CV) of T/C ratio at 6.25 ng/mL (CV = 12.8%) and 100 ng/mL (CV = 7.4%) were both below 15% (Fig. S5). Our nanozyme chemiluminescence strip tests show satisfactory reproducibility.

Moreover, the nanozyme chemiluminescence strip specifically recognized the SARS-CoV-2 spike antigen, while it remained unresponsive to the spike proteins of other human coronaviruses, such as SARS-CoV, MERS-CoV, HCoV-HKU1 and HCoV-OC43 (Fig. 4D). While SARS-CoV-2 shares more than 60% similarities with SARS-CoV, MERS-CoV, HCoV-HKU1 as well as HCoV-OC43 (cause common flu) identified by genome sequence analysis (Liu et al. 2020), our results showed that there was no cross reaction with these coronaviruses in our tests.

3.5. Rapid testing of pseudo-SARS-CoV-2

To verify the validity of our paper test for virus samples, we assessed
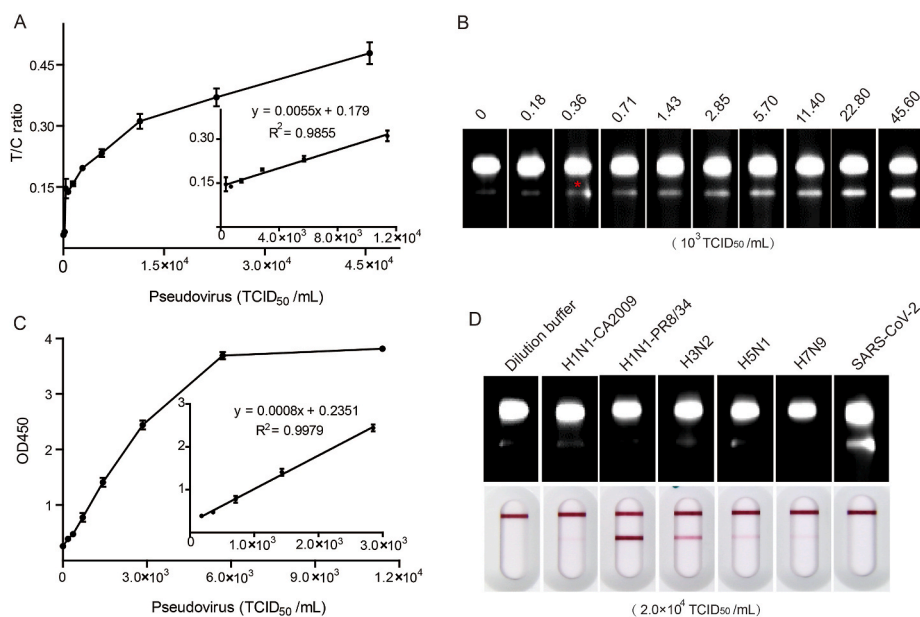
its performance using the pseudo-SARS-CoV-2 expressing spike protein. Gradient dilution series of pseudovirus were detected by the nanozyme chemiluminescence strip. As shown in Fig. 5A and B, the detection limit of chemiluminescence paper test for pseudo-SARS-CoV-2 was approx. 360 TCID$_{50}$/mL. The linearity of the paper test ranged from 360 TCID$_{50}$/mL to 1.14×10^3 TCID$_{50}$/mL (R^2 = 0.9855) (Fig. 5A). In the parallel test, the sensitivity of ELISA reached 360 TCID$_{50}$/mL, with a relatively narrow linear range (from 360 to 2850 TCID$_{50}$/mL) (Fig. 5C).

To evaluate the selectivity of our strip in virus detection, we further tested several influenza A subtypes, including H1N1, H3N2, H5N1 and H7N9. As shown in Fig.5D, our strips recognized pseudo-SARS-CoV-2 specifically, and there was no cross reaction with influenza A subtypes. These inactivated virus samples of influenza A subtypes with the same titer (2×10^4 TCID$_{50}$/mL) were positively tested using the commercial Influenza A antigen detection cards (colloidal gold), which confirmed the antigenicity of the inactivated samples. The results demonstrated that our nanozyme chemiluminescence strip test shows high specificity for SARS-CoV-2.

4. Discussion

Here, we present a novel nanozyme-based chemiluminescence paper test for SARS-CoV-2 antigen detection. In this study, we successfully integrated nanozyme-catalytic chemiluminescence with a lateral immunochromatographic system to achieve sensitive as well as rapid field testing for SARS-CoV-2 antigen, which should greatly benefit the early screening and diagnosis of COVID-19.

Point-of-care tests (POCTs) for viral antigen would be greatly beneficial for early diagnosis of SARS-CoV-2 infection. There is a high requirement for sensitivity in antigen testing due to the low viral load in the early stages of infection. Several antigen rapid tests have been reported (Cerutti et al. 2020; Porte et al. 2020; Scohy et al. 2020). Traditional antigen tests have been developed principally based on colloidal gold immunoassay or fluorescent immunochromatography. There has been a concerted effort to improve the sensitivity and accuracy of antigen test. In this work, the chemiluminescence signal amplification represents a significant improvement in the sensitivity of paper test compared to conventional colloidal gold or fluorescent strip. While the colloidal gold test is based on the color signal of Au nanoparticles, our test is based on nanozyme-catalytic chemiluminescence signal amplification. Our results clearly demonstrated that the sensitivity of

Fig. 4. Rapid testing of recombinant SARS-CoV-2 spike antigen. (A) Gradient paper testing of SARS-CoV-2 S-RBD protein, before and after adding luminol substrate. A total of 100 µl sample solution was loaded for each test. (B) The calibration curve of SARS-CoV-2 S-RBD detection by nanozyme chemiluminescence test strip. The Y value was defined as the chemiluminescent intensity ratio of T-line to C-line. Concentrations of S-RBD protein ranged from 0~6400 ng/mL. Samples were measured in triplicates. (C) Calibration curve of ELISA detection for S-RBD protein. Samples were measured in triplicates. (D) Nanozyme chemiluminescence test paper specifically recognized the spike antigen of SARS-CoV-2, remaining negative for other human coronaviruses (SARS, MERS, HCoV-HKU1 and HCoV-OC43).

Fig. 5. Rapid testing of pseudo-SARS-CoV-2. (A) Calibration curve of pseudovirus test. (B) Gradient detection of pseudo-SARS-CoV-2 samples using nanozyme chemiluminescence test paper. (C) ELISA detection of the pseudo-SARS-CoV-2 samples. Samples were measured in triplicates. (D) Nanozyme chemiluminescence strip specifically recognized the pseudo-SARS-CoV-2. The inactivated samples of H1N1, H3N2, H5N1 and H7N9 with the same titer were tested positively using the commercial Influenza A antigen testing kits.

our test for spike antigen is comparable to that of an ELISA method, which has been considered more sensitive than colloidal gold strip (Jiang et al. 2011; Ling et al. 2015). The detection limit for pseudovirus in our test reached 360 TCID$_{50}$/ml, which is close to the sensitivity of Quidel Sofia antigen test card (USA) (113–226 TCID$_{50}$/mL) and that of ReBio test kit (Japan) (1000 TCID$_{50}$/mL). Critically, the high sensitivity of antigen detection might lower the false negative rate in the early screenings of SARS-CoV-2 infection.

In addition, we established a novel detection platform which is highly suitable for POCT. We integrated nanozyme-catalysis, lateral flow immunoassay, with chemiluminescence sensing together for the first time. Our test is rapid and easy to implement. On average, our paper test can be completed within 16 min, which is faster than either nucleic acid testing (0.5–2 h) or ELISA method (1–2 h). The test can be operated without requirement for skilled personnel or a dedicated site, thus it is suitable for use at the bedside, in communities as well as in open public places. The test can be performed using a portable device or a smartphone, making it available and convenient for field use. In contrast, the traditional chemiluminescence detection depends on large and expensive instruments, which are only applicable for the central laboratory or inspection agency. Therefore, our approach of rapid antigen test is more applicable to field rapid screening.

Importantly, we replaced natural HRP with a Co–Fe@hemin-peroxidase nanozyme in our test. HRP and alkaline phosphatase are the core materials in traditional chemiluminescence immunodiagnosis (Zhang et al. 2018). These natural enzymes are unstable, complex to produce and high-cost. In our study, we have verified that Co–Fe@hemin nanozyme is far more robust for high-temperature and alkaline conditions compared with HRP. Thus, the nanozyme chemiluminescence test paper can be stored stably at ambient temperature, benefiting transportation and field application. Furthermore, Co–Fe@hemin-peroxidase nanozyme catalyzed chemiluminescence as efficiently as HRP. In previous studies, peroxidase activities of the vast majority of nanozymes were lower than HRP. While one previous study reported that Prussian Blue nanoparticles possess peroxidase activity superior to HRP (Komkova et al. 2018), this activity sharply decreases in alkaline condition required for chemiluminescence catalysis according to our investigation. The high chemiluminescent catalytic activity of Co–Fe@hemin-peroxidase nanozyme is vital to the sensitivity of our paper test.

Moreover, Co–Fe@hemin nanozyme can be synthesized from simple

and readily available materials, and is easily scaled up without requiring expensive equipment. Nanozyme is relatively low-cost compared with natural HRP, which requires complex extraction and purification. Accordingly, the overall cost of nanozyme chemiluminescence strip test is relatively low. We estimate that the cost for manufacturing and testing of our strip is approximately RMB 6 yuan (0.9$) per test. The price of the BinaxNOW COVID-19 Ag Card of Abbott is 5$ per test. In contrast, the cost of nucleic acid test is RMB 150 yuan (22.4$) per test in China. This cost advantage may considerably lower the financial burden on national healthcare resources, and critically, benefit regions of low socio-economic standing.

While our study clearly showed that our test is sensitive for recombinant antigen and pseudovirus, it is critical to further validate the accuracy of our strip for real clinical samples, such as saliva or nasal swab specimens. At the time of our investigation, only a few antigen test kits were approved by FDA or have passed European Union certification; however, the officially authorized reagents for rapid testing of SARS-CoV-2 antigen remains unavailable in China, thus parallel comparisons of commercial kits with our test paper in clinical sample detection require future investigation. Lastly, a quantitative test should be developed. A portable handheld device equipped with signal acquisition and data analysis function for our nanozyme chemiluminescence paper test is currently being developed.

5. Conclusions

In conclusion, our nanozyme chemiluminescence paper test combines the high-sensitivity of chemiluminescence, high-specificity of immunoassay, rapid and convenient features of paper test in antigen detection. Our test provides a novel point-of-care approach for early screening of SARS-CoV-2 infections, and should greatly contribute to cost control. Moreover, as a universal paper-based POCT technique, it has promising potential for screening or diagnosing other future infectious diseases with pandemic potential. However, the tests for clinical samples remain to be verified in future research.

CRediT authorship contribution statement

Dan Liu: Conceptualization, Methodology, Investigation, Writing the manuscript. **Chenhui Ju:** Methodology, Investigation, Data analysis. **Chao Han:** Methodology, Antibody development. **Rui Shi:**

Methodology, Investigation. **Xuehui Chen:** Investigation, Data analysis. **Demin Duan:** Conceptualization, Methodology. **Jinghua Yan:** Methodology, Resources, Funding acquisition.

Declaration of competing interest

The authors declare that they have no known competing financial interests or personal relationships that could have appeared to influence the work reported in this paper.

Acknowledgments

Appendix A. Supplementary data

Supplementary data to this article can be found online at https://doi.org/10.1016/j.bios.2020.112817.

References

Amanat, F., Stadlbauer, D., Strohmeier, S., Nguyen, T.H.O., Chromikova, V., McMahon, M., Jiang, K.J., Arunkumar, G.A., Jurczyszak, D., Polanco, J., Bermudez-Gonzalez, M., Kleiner, G., Aydillo, T., Miorin, L., Fierer, D.S., Lugo, L.A., Kojic, E.M., Stoever, J., Liu, S.T.H., Cunningham-Rundles, C., Felgner, P.L., Moran, T., Garcia-Sastre, A., Caplivski, D., Cheng, A.L.C., Kedzierska, K., Vapalahti, O., Hepojoki, J.M., Simon, V., Krammer, F., 2020. Nat. Med. https://doi.org/10.1038/s41591-020-0913-5.

Cerutti, F., Burdino, E., Milia, M.G., Allice, T., Gregori, G., Bruzzone, B., Ghisetti, V., 2020. J. Clin. Virol. 132, 104654.

Cheng, N., Song, Y., Zeinhom, M.M.A., Chang, Y.C., Sheng, L., Li, H.L., Du, D., Li, L., Zhu, M.J., Luo, Y.B., Xu, W.T., Lin, Y.H., 2017. Acs Appl Mater Inter 9 (46), 40671–40680.

Deng, H., Li, X.L., Peng, Q., Wang, X., Chen, J.P., Li, Y.D., 2005. Angew. Chem. Int. Ed. 44 (18), 2782–2785.

Deng, J., Yang, M., Wu, J., Zhang, W., Jiang, X., 2018. Anal. Chem. 90 (15), 9132–9137.

Duan, D., Fan, K., Zhang, D., Tan, S., Liang, M., Liu, Y., Zhang, J., Zhang, P., Liu, W., Qiu, X., Kobinger, G.P., Gao, G.F., Yan, X., 2015. Biosens. Bioelectron. 74, 134–141.

Gao, L.Z., Zhuang, J., Nie, L., Zhang, J.B., Zhang, Y., Gu, N., Wang, T.H., Feng, J., Yang, D.L., Perrett, S., Yan, X., 2007. Nat. Nanotechnol. 2 (9), 577–583.

Grant, P.R., Turner, M.A., Shin, G.Y., Nastouli, E., Levett, L.J., 2020. bioRxiv. https://doi.org/10.1101/2020.04.06.028316.

Hu, B., Guo, H., Zhou, P., Shi, Z.L., 2020. Nat. Rev. Microbiol.

Huang, W.E., Lim, B., Hsu, C.C., Xiong, D., Wu, W., Yu, Y.J., Jia, H.D., Wang, Y., Zeng, Y. D., Ji, M.M., Chang, H., Zhang, X.M., Wang, H., Cui, Z.F., 2020. Microb Biotechnol. https://doi.org/10.1111/1751-7915.13586.

Jia, X., Zhang, P., Tian, Y., Wang, J., Zeng, H., Wang, J., Liu, J., Chen, Z., Zhang, L., He, H., He, K., Liu, Y., 2020. bioRxiv. https://doi.org/10.1101/2020.1102.1128.20029025.

Jiang, B., Duan, D., Gao, L., Zhou, M., Fan, K., Tang, Y., Xi, J., Bi, Y., Tong, Z., Gao, G.F., Xie, N., Tang, A., Nie, G., Liang, M., Yan, X., 2018. Nat. Protoc. 13 (7), 1506–1520.

Jiang, J., Wang, Z., Zhang, H., Zhang, X., Liu, X., Wang, S., 2011. J. Agric. Food Chem. 59 (18), 9763–9769.

Komkova, M.A., Karyakina, E.E., Karyakin, A.A., 2018. J. Am. Chem. Soc. 140 (36), 11302–11307.

Li, Q.Q., Wu, J.J., Nie, J.H., Zhang, L., Hao, H., Liu, S., Zhao, C.Y., Zhang, Q., Liu, H., Nie, L.L., Qin, H.Y., Wang, M., Lu, Q., Li, X.Y., Sun, Q.Y., Liu, J.K., Zhang, L.Q., Li, X. G., Huang, W.J., Wang, Y.C., 2020a. Cell 182 (5), 1284–+.

Li, Z., Yi, Y., Luo, X., Xiong, N., Liu, Y., Li, S., Sun, R., Wang, Y., Hu, B., Chen, W., Zhang, Y., Wang, J., Huang, B., Lin, Y., Yang, J., Cai, W., Wang, X., Cheng, J., Chen, Z., Sun, K., Pan, W., Zhan, Z., Chen, L., Ye, F., 2020b. J. Med. Virol. https://doi.org/10.1002/jmv.25727.

Ling, S., Chen, Q.A., Zhang, Y., Wang, R., Jin, N., Pang, J., Wang, S., 2015. Biosens. Bioelectron. 71, 256–260.

Liu, Y., Liu, B., Cui, J., Wang, Z., Shen, Y., Xu, Y., Yao, K., Guan, Y., 2020. Preprints. https://doi.org/10.20944/preprints202003.200316.v202001.

Ma, J., Chen, R.F., Huang, W.J., Nie, J.H., Liu, Q., Wang, Y.C., Yang, X.M., 2019. Hum. Vaccines Immunother. 15 (10), 2286–2294.

Mei, X., Lee, H.C., Diao, K.Y., Huang, M., Lin, B., Liu, C., Xie, Z., Ma, Y., Robson, P.M., Chung, M., Bernheim, A., Mani, V., Calcagno, C., Li, K., Li, S., Shan, H., Lv, J., Zhao, T., Xia, J., Long, Q., Steinberger, S., Jacobi, A., Deyer, T., Luksza, M., Liu, F., Little, B.P., Fayad, Z.A., Yang, Y., 2020. Nat. Med. 26 (8), 1224–1228.

Nie, J.H., Li, Q.Q., Wu, J.J., Zhao, C.Y., Hao, H., Liu, H., Zhang, L., Nie, L.L., Qin, H.Y., Wang, M., Lu, Q., Li, X.Y., Sun, Q.Y., Liu, J.K., Fan, C.F., Huang, W.J., Xu, M., Wang, Y.H., 2020. Emerg. Microb. Infect. 9 (1), 680–686.

Oie, A.H.S., 2015. J.B.O.I.D.É. 1092–1106.

Porte, L., Legarraga, P., Vollrath, V., Aguilera, X., Munita, J.M., Araos, R., Pizarro, G., Vial, P., Iruretagoyena, M., Dittrich, S., Weitzel, T., 2020. Int. J. Infect. Dis. 99, 328–333.

Scohy, A., Anantharajah, A., Bodeus, M., Kabamba-Mukadi, B., Verroken, A., Rodriguez-Villalobos, H., 2020. J. Clin. Virol. 129, 104455.

Shi, R., Shan, C., Duan, X., Chen, Z., Liu, P., Song, J., Song, T., Bi, X., Han, C., Wu, L., Gao, G., Hu, X., Zhang, Y., Tong, Z., Huang, W., Liu, W.J., Wu, G., Zhang, B., Wang, L., Qi, J., Feng, H., Wang, F.S., Wang, Q., Gao, G.F., Yuan, Z., Yan, J., 2020a. Nature. https://doi.org/10.1038/s41586-020-2381-y.

Shi, Y., Wang, Y., Shao, C., Huang, J., Gan, J., Huang, X., Bucci, E., Piacentini, M., Ippolito, G., Melino, G., 2020b. Cell Death Differ. 27 (5), 1451–1454.

Who, 2020. Antigen-detection in the Diagnosis of SARS-CoV-2 Infection Using Rapid Immunoassays. https://apps.who.int/iris/bitstream/handle/10665/334253/WHO-2019-nCoV-Antigen_Detection-2020.1-eng.pdf?sequence=1&isAllowed=y.

Wiersinga, W.J., Rhodes, A., Cheng, A.C., Peacock, S.J., Prescott, H.C., 2020. JAMA, J. Am. Med. Assoc. 324 (8), 782–793.

Wrapp, D., Wang, N.S., Corbett, K.S., Goldsmith, J.A., Hsieh, C.L., Abiona, O., Graham, B. S., McLellan, J.S., 2020. Science 367 (6483), 1260–+.

Wu, F., Zhao, S., Yu, B., Chen, Y.M., Wang, W., Song, Z.G., Hu, Y., Tao, Z.W., Tian, J.H., Pei, Y.Y., Yuan, M.L., Zhang, Y.L., Dai, F.H., Liu, Y., Wang, Q.M., Zheng, J.J., Xu, L., Holmes, E.C., Zhang, Y.Z., 2020. Nature 579 (7798), 265–+.

Xiao, S.Y., Wu, Y., Liu, H., 2020. J. Med. Virol. 92 (5), 464–467.

Zhang, Z., Lai, J.H., Wu, K.S., Huang, X.C., Guo, S., Zhang, L.L., Liu, J., 2018. Talanta 180, 260–270.

Zhao, J., Yuan, Q., Wang, H., Liu, W., Liao, X., Su, Y., Wang, X., Yuan, J., Li, T., Li, J., Qian, S., Hong, C., Wang, F., Liu, Y., Wang, Z., He, Q., Li, Z., He, B., Zhang, T., Fu, Y., Ge, S., Liu, L., Zhang, J., Xia, N., Zhang, Z., 2020. Clin. Infect. Dis. https://doi.org/10.1093/cid/ciaa1344.

Zhou, P., Yang, X.L., Wang, X.G., Hu, B., Zhang, L., Zhang, W., Si, H.R., Zhu, Y., Li, B., Huang, C.L., Chen, H.D., Chen, J., Luo, Y., Guo, H., Jiang, R.D., Liu, M.Q., Chen, Y., Shen, X.R., Wang, X., Zheng, X.S., Zhao, K., Chen, Q.J., Deng, F., Liu, L.L., Yan, B., Zhan, F.X., Wang, Y.Y., Xiao, G.F., Shi, Z.L., 2020. Nature 579 (7798), 270–+.

Zhuang, J., Fan, K., Gao, L., Lu, D., Feng, J., Yang, D., Gu, N., Zhang, Y., Liang, M., Yan, X., 2012. Mol. Pharm. 9 (7), 1983–1989.